Synthesis and evaluation of the potential deleterious effects of ZnO nanomaterials (nanoneedles and nanoflowers) on blood components, including albumin, erythrocytes and human isolated primary neutrophils

Bruna Pastrello, Luana Chiquetto Paracatu, Luiza de Carvalho Bertozo, Iêda Maria Martinez Paino, et al.

Journal of Nanoparticle Research
An Interdisciplinary Forum for
Nanoscale Science and Technology

ISSN 1388-0764
Volume 18
Number 7

J Nanopart Res (2016) 18:1-12
DOI 10.1007/s11051-016-3527-6

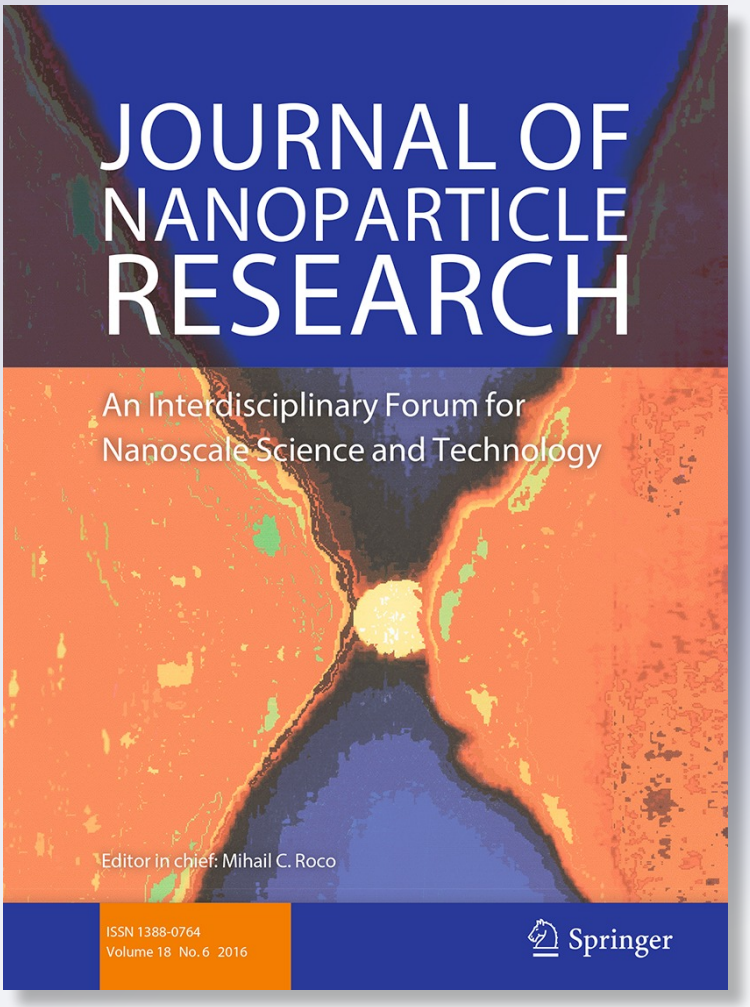

Springer

J Nanopart Res (2016)18:216
DOI 10.1007/s11051-016-3527-6

RESEARCH PAPER

Synthesis and evaluation of the potential deleterious effects of ZnO nanomaterials (nanoneedles and nanoflowers) on blood components, including albumin, erythrocytes and human isolated primary neutrophils

Bruna Pastrello · Luana Chiquetto Paracatu · Luiza de Carvalho Bertozo · Iêda Maria Martinez Paino · Paulo Noronha Lisboa-Filho · Valdecir Farias Ximenes

Received: 23 March 2016 / Accepted: 20 July 2016

Abstract The application of zinc oxide (ZnO) nanoparticles in biomaterials has increased significantly in the recent years. Here, we aimed to study the potential deleterious effects of ZnO on blood components, including human serum albumin (HSA), erythrocytes and human isolated primary neutrophils. To test the influence of the morphology of the nanomaterials, ZnO nanoneedles (ZnO-nn) and nanoflowers (ZnO-nf) were synthesized. The zeta potential and mean size of ZnO-nf and ZnO-nn suspensions in phosphate-buffered saline were −10.73 mV and 3.81 nm and −5.27 mV and 18.26 nm, respectively. The incubation of ZnO with HSA did not cause its denaturation as verified by the absence of significant alterations in the intrinsic and extrinsic fluorescence and in the circular dichroism spectrum of the protein. The capacity of HSA as a drug carrier was not affected as verified by employing site I and II fluorescent markers. Neither type of ZnO was able to provoke the activation of neutrophils, as verified by lucigenin- and luminol-dependent chemiluminescence and by the extracellular release of hydrogen peroxide. ZnO-nf, but not ZnO-nn, induced the haemolysis of erythrocytes. In conclusion, our results reinforce the concept that ZnO nanomaterials are relatively safe for usage in biomaterials. A potential exception is the capacity of ZnO-nf to promote the lysis of erythrocytes, a discovery that shows the importance of the morphology in the toxicity of nanoparticles.

Keywords Erythrocytes · Human serum albumin · Neutrophils · Sonochemistry · Zinc oxide nanoparticles · Metal oxide nanoparticles · Health effects

B. Pastrello · L. de Carvalho Bertozo · V. F. Ximenes (✉)
Department of Chemistry, Faculty of Sciences, São Paulo State University (UNESP), P.O. Box 473, Bauru, São Paulo 17033-360, Brazil
e-mail: vfximenes@fc.unesp.br

L. C. Paracatu
Department of Clinical Analysis, School of Pharmaceutical Sciences, São Paulo State University (UNESP), Araraquara, São Paulo 14801-902, Brazil

I. M. M. Paino
Nanomedicine and Nanotoxicology Group, Physics Institute of São Carlos (IFSC), University of São Paulo (USP), São Carlos, São Paulo 13560-970, Brazil

P. N. Lisboa-Filho
Department of Physics, Faculty of Sciences, São Paulo State University (UNESP), Bauru, São Paulo 17033-360, Brazil

Introduction

The number of studies dedicated to the potential harmful effects of nanostructured material has increased in line with those showing new and beneficial applications of these materials. In particular, for metal oxide nanoparticles (NPs), which are already

Published online: 30 July 2016

produced at an industrial scale, concerns about their toxicities are a hot topic (Djurišić et al. 2015; Sarkar et al. 2014). Zinc oxide (ZnO) NPs have received special attention, since besides their wide usage in electronics devices, paints, cosmetic, etc., many new applications have been described in which direct contact of this material with the human body is implicit or proposed (Roy et al. 2015; Madhumitha et al. 2015). A few examples of recent applications include the conjugation of ZnO NPs with a natural extract of Red Sandalwood, which was demonstrated as a potent anti-diabetic agent (Kitture et al. 2015); the application of nanocomplexes formed by the incorporation of ZnO NPs into liposomes as a pH-responsive drug delivery system for the release of daunorubicin (Tripathy et al. 2015); ZnO-porphyrin NPs as a potential alternative for treatment of various cancers in photodynamic therapy (Sadjadpour et al. 2015) and the synthesis of carboxymethyl cellulose/ZnO nanocomposite hydrogels and their antibacterial effects against *Escherichia coli* and *Staphylococcus aureus* (Yadollahi et al. 2015). Particularly relevant in the context of this work is the capacity of ZnO to trigger the inflammatory process, including the capacity of ZnO NPs to provoke eosinophilic airway inflammation in mice exposed to different concentrations of ZnO (Huang et al. 2015); the induction of acute pulmonary dysfunction and inflammation (Fukui et al. 2015); activation of extracellular signal-regulated kinase (ERK) leading to expression and secretion of tumour necrosis factor (TNF)-α in human keratinocytes (Jeong et al. 2013) and induction of significant up-regulation of mRNA for the proinflammatory cytokine interleukin (IL)-8 and redox stress marker haem oxygenase-1 in human lung epithelial cells (Saptarshi et al. 2015). In cell culture studies, the toxic effect of ZnO NPs has been also demonstrated. For instance, the capacity of silver, TiO_2 and ZnO NPs at ultralow levels as inductors of proinflammatory responses in RAW264.7 macrophages (Giovanni et al. 2015). The cytotoxic effect of ZnO NPs in 3D cell culture system using colon cell spheroids showed that conclusions made from 2D cell models might overestimate the toxicity of ZnO NPs (Chia et al. 2015). Regarding the toxic effect on intestinal cells, ZnO NPs was also most toxic compared to silicon dioxide (SiO_2) and TiO_2 (Setyawati et al. 2015a).

In this study, we examined the potential deleterious effects of ZnO nanomaterials on the blood components, including the major serum protein, albumin and the main cell constituents, erythrocytes and human isolated primary neutrophils. Particularly, we were also interested in the differential effects related to the shape of the ZnO NPs, here evaluated for nanoflowers and nanoneedles morphologies. In this concern, as highlighted by Tay et al. (2014), besides the size, the shape of nanomaterials has also been shown to affect the cellular response.

This line of investigation was motivated by the well-accepted knowledge that irrespective of their function and target tissue, a nanomaterial engineered for application in nanomedicine will have contact with the blood vessels and cells. For instance, Setyawati et al. (2015b) recently published a review regarding the importance of the study of the interaction and toxic effects of nanomaterials with endothelial cells. In the literature, there is much evidence that metal oxide NPs are able to interact with leukocytes. For instance, TiO_2, CeO_2 and ZnO promote the expression and release of enzymes that play important roles in the innate immune system, such as myeloperoxidase, MMP-9 and gelatinase in neutrophils (Babin et al. 2013). ZnO NPs increased the neutrophil size, induced shape changes and activated phosphorylation events (Gonçalves and Girard 2014). Monocytes exposed to ZnO NPs increased the release of proinflammatory cytokines IL-1β, TNF-α and IL-6, as well as chemokine IL-8 (Sahu et al. 2014).

Materials and methods

Chemical and solutions

Zinc acetate dehydrate, human serum albumin (HSA) free of fatty acids (A1887), dansylglycine, dansylamide, 8-anilino-1-naphthalene sulphonic acid, luminol, lucigenin, dansylglycine, dansylamide, Histopaque 1077/1119 and phorbol myristate acetate were obtained from Sigma-Aldrich Chemical Co. (St. Louis, MO, USA). 10-Acetyl-3,7-dihydroxyphenoxazine (Amplex Red) was obtained from Santa Cruz Biotechnology (Santa Cruz, CA, USA). Phosphate-buffered saline (PBS) was prepared by dissolving a commercial tablet (Sigma-Aldrich) and adjusting the pH to 7.4. All reagents used for solution and buffer preparations were of analytical grade. All solutions were prepared with water purified by a Milli-Q system (Millipore, Bedford, MA, USA).

Synthesis and characterization of ZnO nanomaterials

Zinc nanostructures were prepared as follows: 2.75 g of zinc acetate dehydrate [$Zn(CH_3COO^-)_2 \cdot 2H_2O$] was dissolved in 25 mL of aqueous ammonium solution (NH_3, 25 %). Sodium hydroxide (1 g) was added and the suspension was stirred until complete dissolution of NaOH. Two suspensions were prepared and submitted to sonochemical treatment for 10 or 60 min using an amplitude of 40 % and an effective power of 25 W in a 20-kHz, 750-W Sonics VCX-750 ultrasonic processor (Hielscher Ultrasonics, Teltow, Germany). After this treatment, these suspensions were left to rest. The precipitates were collected and washed four times in deionized water using a Z-326 centrifuge (Hermle Labortechnik, Wehingen, Germany) in 15-min cycle at 12,000 rpm. Finally, the precipitates were dried in a muffle furnace and air atmosphere at 200 °C for 2 h. The identification of crystallographic phases of ZnO was performed by X-ray diffraction using a RIGAKU D/MAX 2100 PC diffractometer. UV–Vis absorption measurements were used for the evaluation of the nanostructured ZnO band gap. For these experiments, ethanolic suspensions of ZnO (0.1 mg/mL) were scanned in the wavelength range of 250–500 nm using a UV–Vis Lambda 35 spectrophotometer (Perkin Elmer, Shelton, CT, USA). The morphology and shape of the prepared nanoparticles were analysed by field emission scanning electron microscopy (FE-SEM) using a Sigma series ZEISS microscope model (Germany). The hydrodynamic diameter (average size) and zeta potential of nanomaterials suspended in PBS were determined using dynamic light scattering (DLS, Malvern instruments®, UK).

Studies of the effects of ZnO on human serum albumin

The suspensions were composed of ZnO (0.1 mg/mL) and 10 μM HSA in PBS. The samples were gently homogenized while being incubated for 24 h at 37 °C using a blood-tube rotator. Then, the samples were centrifuged at 1000*g* for remotion of ZnO. The protein in the supernatant was isolated for subsequent studies. The intrinsic fluorescence spectra of HSA were obtained using a Perkin Elmer LS 55 spectrofluorimeter (Shelton, CT, USA). The parameters were as follows: excitation at 295 nm and emission in the range of 310–450 nm. The slit widths were 5 nm for excitation and 5 nm for emission wavelengths. The analyses were performed using a 10-mm path length in a 3-mL quartz cuvette. The samples were magnetically stirred during the measurements. The synchronous fluorescence spectra were obtained by simultaneously scanning the excitation and emission monochromators. A fixed $\Delta\lambda$ of 15 nm was kept to assess the alteration near the tyrosine residues and $\Delta\lambda$ of 60 nm for alteration near the tryptophan residue in HSA.

8-Anilino-1-naphthalene sulfonic acid fluorescence measurements were performed by adding 10 μM of this compound after the treatment of HSA with ZnO nanoparticles as described above. The spectrofluorimeter was adjusted as follows: excitation at 340 nm, emission scanning between 410 and 600 nm and a slit width of 5.0 nm for both excitation and emission wavelengths. Similarly, dansylamide (DNSA) and dansylglycine (DG) fluorescence measurements were performed by adding 10 μM of these compounds after treating HSA with ZnO nanoparticles. The spectrofluorimeter was adjusted as follows: excitation at 340 nm, emission scanning between 410 and 600 nm and slit width of 5.0 nm for both excitation and emission wavelengths.

Circular dichroism (CD) spectra were recorded with a Jasco J-815 spectropolarimeter (Jasco, Japan) equipped with a thermostatically controlled cell holder at 25 °C. The spectra were accumulated in duplicate with 1-nm step resolution at a scanning speed of 50 nm/min and a path length cell of 1.0 mm. The baseline (PBS) was subtracted from all measurements. Before the measurements, the samples (treated as indicated above) were centrifuged at 1000*g* for remotion of ZnO and diluted to a final concentration of 1 μM HSA.

Isolation of human primary neutrophils

Blood samples were taken from healthy volunteers according to the protocol approved by the University of the State of São Paulo Ethics Committee (CEP/FCF-UNESP No. 40979014.2.0000.5398). Neutrophils were isolated by a double density-gradient centrifugation technique (700*g*, 30 min, 25 °C) using Histopaque-1077 and 1119 as indicated by the manufacturer (Sigma-Aldrich). The supernatant was discarded and the neutrophils were washed twice with

PBS buffer (700*g*, 10 min, 25 °C). The neutrophils were counted and suspended in PBS supplemented with 0.5 mM $CaCl_2$, 0.5 mM $MgCl_2$ and 1 mg/mL glucose (Paracatu et al. 2014).

Studies of the effects of ZnO on neutrophils by chemiluminescence assays

Assays were performed as previously described with modifications (de Faria et al. 2012).

Lucigenin assay

The reaction medium was composed of neutrophils (2×10^6 cells/mL), ZnO nanoparticles (0.1 mg/mL) and lucigenin (10 μM) in supplemented PBS. ZnO was absent in the negative control and was replaced with PMA (100 nM) in the positive control. The reactions were performed in a microplate (final volume: 250 μl) and triggered by adding ZnO or PMA. The light emission was monitored for 30 min at 37 °C using a Centro LB 960 microplate luminometer (Berthold Technologies, Oak Ridge, TN, USA).

Luminol assay

This assay was similar to that described above, except that lucigenin was replaced with 100 μM luminol. Each experiment was repeated at least three times with different cell batches.

Studies of the effect of ZnO on neutrophils using the Amplex Red assay

Assays were performed as previously described with modifications (Zhou et al. 1997). The reaction medium was composed of fresh isolated primary human neutrophils (2×10^6 cells/mL), ZnO nanoparticles (0.1 mg/mL) and Amplex Red (50 μM) in supplemented PBS. ZnO was absent in the negative control and was replaced with PMA (100 nM) in the positive control. The reactions were performed in microcentrifuge tubes (final volume: 300 μl) and triggered by adding ZnO or PMA. The samples were homogenized while being incubated for 30 h at 37 °C using a blood-tube rotator. Next, the samples were centrifuged at 700*g* for 5 min, the supernatant (250 μL) was transferred to a 96-well microplate and the fluorescence was measured at 530/590 nm using a microplate reader (Synergy 2; BioTek, Winooski, VT, USA).

Haemolysis assay

Assays were performed as previously described with modifications (Ximenes et al. 2010). Human erythrocytes from healthy donors were obtained from peripheral blood, centrifuged at 770*g* for 10 min and washed three times with PBS. The supernatant and buffy coat were removed by aspiration after each wash. The cells were resuspended to 20 % (v/v) in PBS. The erythrocytes suspensions (500 μL) were added to 500 μL of 0.1 mg/mL ZnO in PBS and gently homogenized while being incubated for 24 h at 37 °C using a blood-tube rotator. Aliquots (75 μL) were removed and diluted to 1500 μL PBS and centrifuged at 1000*g* for 10 min. The degree of haemolysis was measured in the supernatant by its absorbance at 540 nm. A reference value (100 % haemolysis) was determined with the same aliquot of erythrocytes but diluted in 1500 μL of distilled water instead of PBS to provoke the total lysis of the erythrocytes.

Statistical analysis

The data are reported as mean ± SEM and were analysed by one-way ANOVA and Tukey post-test using GraphPad Prism version 5.00 for Windows (GraphPad Software, San Diego, CA, USA). Statistical significance was established at $p < 0.05$.

Results and discussion

Synthesis and characterizing ZnO nanostructures

The sonochemical synthesis resulted in homogeneous batches of ZnO NPs with the following yields: 77 % (sonication for 10 min) and 99 % (sonication for 40 min). The XRD patterns of the obtained powders showed that both preparations resulted in a polycrystalline ZnO hexagonal phase (Wurtzite—JCPDS 36-1451; Fig. 1a). Furthermore, UV–Vis spectroscopy (Fig. 1b) was used to determine the band gap of the prepared samples, and it was calculated by the Tauc method as 3.3 eV (Fig. 1c), indicating the nanocrystalline nature of the ZnO powder (Janotti and Van de Walle 2009). FE-SEM analyses (Fig. 2a, b)

show that for the samples sonicated for 10 and 40 min, flower-like and needle-like nanostructures were obtained, respectively. These results are similar to the nanostructured morphologies obtained by Khorsand et al. (2013) using a sonochemical method. Zeta potential and hydrodynamic diameter were measured after suspension of the nanostructures in PBS (0.1 mg/mL). The zeta potential and mean size of ZnO nanoflowers were −10.73 mV and 3.81 nm, respectively, and −5.27 mV and 18.26 nm for ZnO nanoneedles, respectively. Figure 3 shows the hydrodynamic diameter of nanoflowers (a) and nanoneedles (b) in PBS.

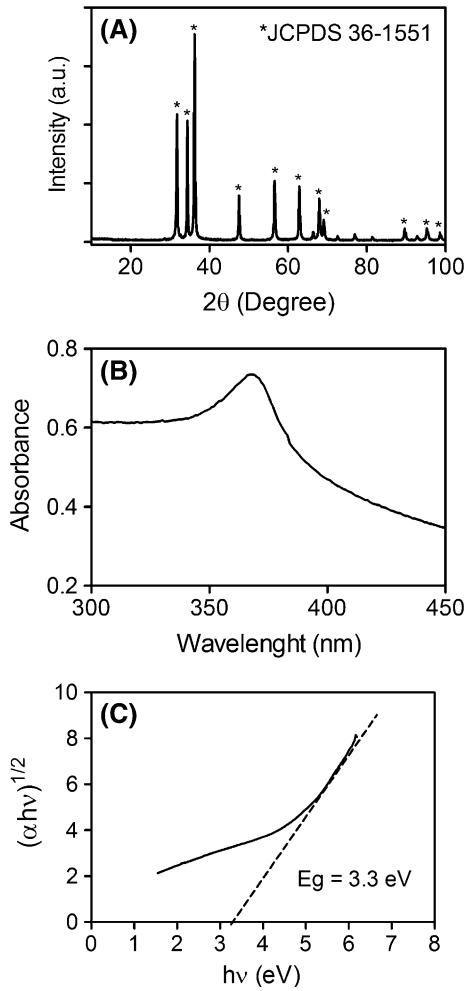

Fig. 1 **a** XRD pattern, **b** UV–visible absorption spectrum of ZnO NPs and **c** variation of $(\alpha h\nu)^{1/2}$ with $h\nu$ for ZnO NPs as a function of wavelength at n value of 1/2

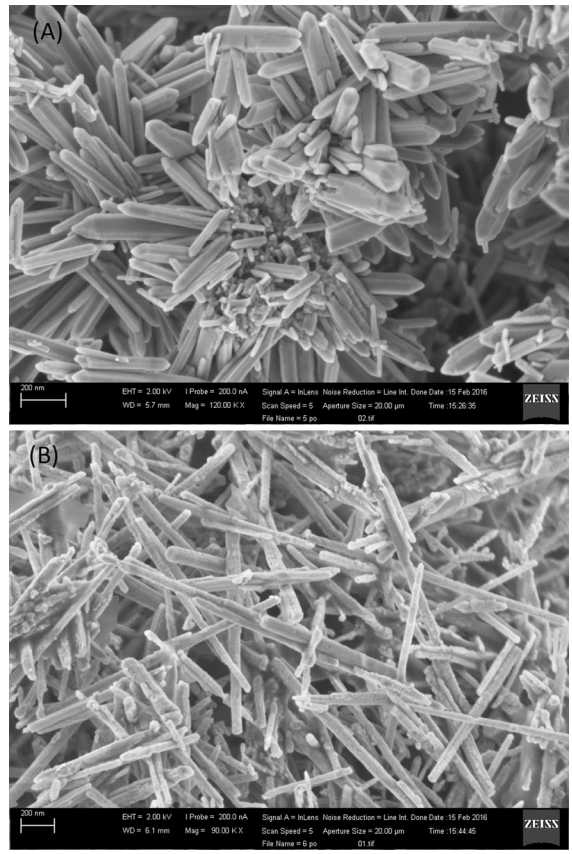

Fig. 2 FE-SEM images of ZnO nanoparticles. **a** Sonication for 10 min (nanoflowers). **b** Sonication for 40 min (nanoneedles)

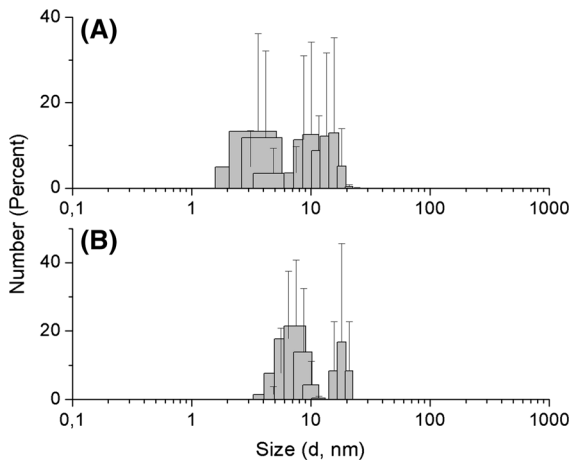

Fig. 3 Hydrodynamic diameter or size distribution by number of nanoflowers (**a**) and nanoneedles (**b**) in PBS. Data are reported as mean ± standard deviation (SD) of triplicate experiments

Studies on structural and functional alterations in HSA

HSA is the major protein in human blood plasma. It has many physiological functions, including the transportation of endogenous and exogenous metabolites and drugs; as a solute for osmotic pressure of blood and as a buffer for pH homoeostasis (Quinlan et al. 2005). For this reason, we evaluated whether the interaction of ZnO nanoneedles or nanoflowers could alter the biophysical properties of HSA. In particular, we were interested in indications of denaturation that were provoked by its prolonged contact with ZnO NPs. These experiments were performed by the incubating 0.1 mg/mL suspensions of ZnO NPs with 10 μM HSA in PBS at 37 °C for 24 h, and then the samples were centrifuged and the measurements were performed using the supernatant. This is an important point because the ZnO NPs are not soluble and provoke turbidity in the medium, which could provoke significant physical quenching of the fluorescence. Therefore, by removing ZnO NPs, any detectable alteration in the intrinsic or extrinsic fluorescence spectra would be related to modifications in the structure of the protein.

How the well-known intrinsic fluorescence spectra of a protein are related to the presence of the aromatic amino acids. In particular, when excited at 295 nm, tryptophan is the main amino acid responsible for the emission (Lakowicz 2006). This was our choice because HSA has only a single tryptophan residue, which is located in the hydrophobic cavity of the IIA subdomain at position 214 in the amino acid sequence, and the emission spectrum is sensitive to its environment (Santra et al. 2004). Hence, any alteration in the tertiary structure of the protein provoked by the interaction with the ZnO NPs could be revealed by alterations in the HSA intrinsic fluorescence. Figure 4a shows the emission spectra of HSA alone or incubated with the nanoparticles. The nanoparticles were not able to induce a significant shift in the maximum fluorescence. In other words, tryptophan 214 experiences the same environment in the protein before and after the contact with ZnO NPs, which is an indication that ZnO NPs were not able to denature HSA.

Another approach to evaluate the structural alterations in proteins is by the measurement of its synchronous fluorescence spectrum. These

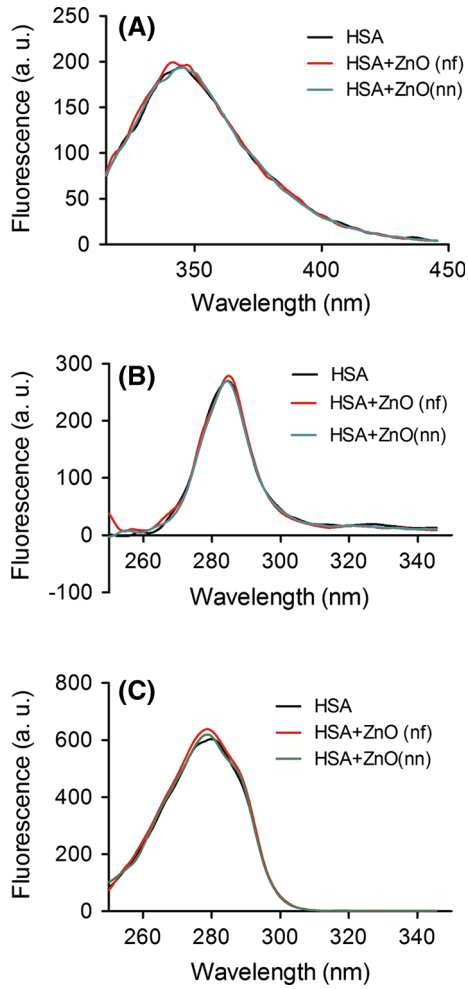

Fig. 4 Studies of structural alterations of HSA induced by ZnO nanoparticles. **a** Intrinsic fluorescence spectra, **b** synchronous fluorescence spectra ($\Delta\lambda = 15$ nm), **c** synchronous fluorescence spectra ($\Delta\lambda = 60$ nm). HSA (10 μM) was incubated with 0.1 mg/mL ZnO nanoflowers (nf) or nanoneedles (nn) for 24 h. The results are representative of at least three experiments

experiments were performed by simultaneously scanning the monochromators with a fixed difference in the wavelength of excitation and emission of 15 or 60 nm. How well-established, the synchronous fluorescence spectra provide information about the microenvironment in a vicinity of the fluorescent amino acids in proteins. Specifically, by monitoring with a $\Delta\lambda = 15$ and $\Delta\lambda = 60$ nm, alterations in the protein structure next tyrosine and tryptophan can be detected, respectively (Miller 1979). The results presented in Fig. 4b, c confirm that ZnO NPs were not able to induce significant alterations in the structure of HSA.

Next, the potential deleterious effects of ZnO NPs on HSA were investigated using fluorescent dyes that are able to characterize alterations in the structure and hydrophobicity of the protein. The first dye was 8-anilino-1-naphthalene sulfonic acid (ANS), a fluorescent probe that has its emission quantum yield increased and the maximum of fluorescence blue-shifted when bound to hydrophobic regions of proteins. This technique has been used for the detection of unfolding of proteins, which exposes previously buried hydrophobic regions of the protein leading to an increase in the ANS fluorescence (Lakowicz 2006). The results depicted in Fig. 5a show the fluorescence of ANS in the absence and presence of HSA. The results also show the blue-shift and increase in quantum yield when ANS is bound to the protein. The contact between the protein and the nanoparticles did not induce any apparent HSA unfolding, since the ANS fluorescence was not significantly altered.

As stated in the beginning of this section, HSA acts as a carrier of drugs in the systemic circulation (Quinlan et al. 2005), and hence, this functional feature of HSA was studied using two fluorescent dyes that are used as binding-site markers in albumin. HSA has two major binding sites for transportation of drugs, referred to as site I and site II, which are located in the hydrophobic cavities of the subdomains IIA and IIIA, respectively. Site I is usually referred to as the warfarin-binding site, whereas site II is designated as the benzodiazepine-binding site (Sudlow et al. 1975). Here, we used the fluorescent compound dansylamide (DA) as a marker of site I and dansylglycine (DG) for characterization of site II (Sudlow et al. 1976; Graciani and Ximenes 2013). Similar to ANS, these fluorescent probes have their quantum yield increased when bound to albumin. We evaluated whether the ZnO NPs could alter the capacity of HSA to use its binding sites, which would be detected by decreased fluorescence of these probes. The results in Fig. 5b, c show that, in agreement with the previous results, the incubation of HSA with ZnO NPs for 24 h did not induce structural alterations that were able to impede the binding of the protein to these compounds. In others words, there is no indication that the contact of ZnO NPs with HSA was able to affect its capacity as drug carrier.

Finally, we measured whether the contact of HSA with the nanoparticles could alter the secondary structure of the protein. These experiments were

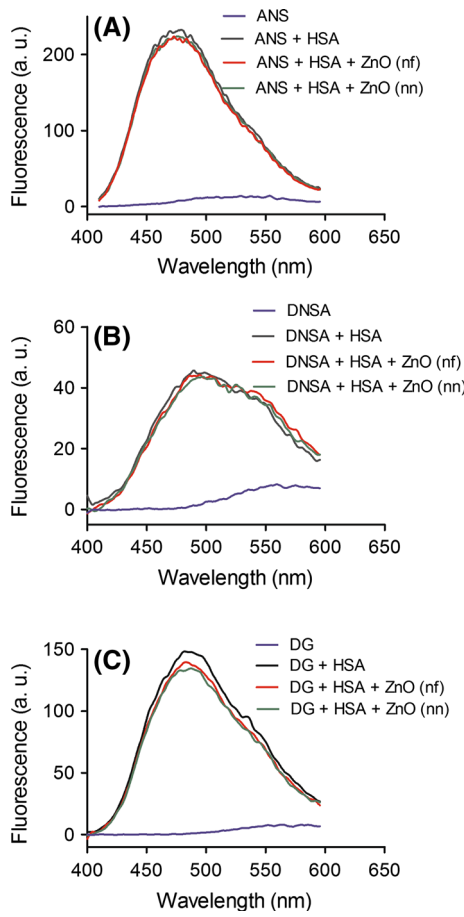

Fig. 5 Studies of unfolding and loss of binding capacity of HSA induced by ZnO nanoparticles. **a** ANS fluorescence as an indication of HSA unfolding. **b** DNSA as an indication of site I binding-site capacity. **c** DG as an indication of site II binding-site capacity. HSA (10 μM) was incubated with 0.1 mg/mL ZnO nanoflowers (nf) or nanoneedles (nn) for 24 h. The results are representative of at least three experiments

performed by measuring the far-UV circular dichroism spectra of the protein before and after incubation with ZnO. Again, it must be emphasized that after incubation, the nanoparticles were removed for centrifugation, otherwise the strong turbidity of the medium would interfere with the measurement. Corroborating the previous results, alterations in the UV-CD spectrum of HSA were not significant (Fig. 6).

In summary, the prolonged contact of ZnO with HSA did not induce significant alterations in the structure of HSA or its capacity to bind site I and II ligands. In disagreement with our findings, Žūkienė and Snitka (2015) demonstrated that ZnO NPs induced conformational changes in bovine serum albumin

(BSA), including a changed microenvironment of the aromatic amino acids. Similarly, Bhogale et al. (2013) demonstrated the formation of BSA–ZnO complexes and conformational changes in BSA. However, their experimental approaches were significantly different, because the spectral properties of the protein were measured in the presence of the nanoparticles, which were covalently or non-covalently bound to the protein. For these reasons, these results cannot be directly compared with ours, in which the nanoparticles were removed before the measurements. Finally, it must be emphasized that in our experimental model, the putative presence of HSA bound to ZnO NPs was not analysed in this work. Obviously, this minor fraction of HSA bound to the protein might be altered as indicated by Žūkienė and Snitka (2015) and Bhogale et al. (2013).

Studies on haemolysis

Another essential component of the blood is the erythrocytes. Our next step was to study the capacity of ZnO NPs to damage the membrane of the erythrocytes, which was evaluated by measuring the release of haemoglobin into the medium, i.e. the haemolysis provoked by the contact with ZnO NPs. In these experiments, 10 % cell suspensions, in the presence or absence of ZnO, NPs were gently homogenized while being incubated for 24 h at 37 °C. A positive control was obtained by changing the PBS buffer for pure water, which provoked the total haemolysis of the cells (100 % haemolysis). The negative control was obtained by homogenizing the sample in the absence of ZnO. Some haemolysis is also obtained during this assay due to the processing of the blood. The results depicted in Fig. 7 show that the ZnO nanoflowers, but not the nanoneedles, were able to provoke a small but statistically significant increase in haemolysis compared to the negative control.

Due to their potential applications, e.g. as drug carriers, there will be contact between the nanoparticles and the erythrocytes and hence, the evaluation of haemolytic activity is an important toxicological parameter for these materials (Pillai et al. 2015; Easo and Mohanan 2015; Ghosh et al. 2013). In particular, for ZnO, Das et al. (2013) demonstrated that using up to 2.5 mg/mL of this material provoked less than 5 % haemolysis. It is of note that, besides the difference in the morphology of the ZnO studied (nanospheres), the source of erythrocytes (sheep) and the higher concentration of ZnO, the cells were incubated for just 90 min, which is significantly lower compared to the 24-h incubation in the present study. This difference could explain the higher level of haemolysis obtained here, where only 0.1 mg/mL was used (11 % nanoneedles and 22 % nanoflowers).

Regarding the higher haemolytic activity of ZnO nanoflowers compared to nanoneedles, as far as we know, this is the first demonstration that this morphology is potentially more cytotoxic regarding haemolysis of erythrocytes. With respect to cytotoxicity, in the literature, there are some studies regarding different morphologies of nanoparticles and their

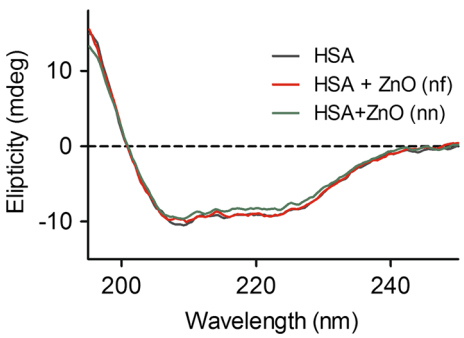

Fig. 6 Studies on alterations of the secondary structure of HSA induced by ZnO nanoparticles. HSA (10 μM) was incubated with 0.1 mg/mL ZnO nanoflowers (nf) or nanoneedles (nn) for 24 h. The results are representative of at least three experiments

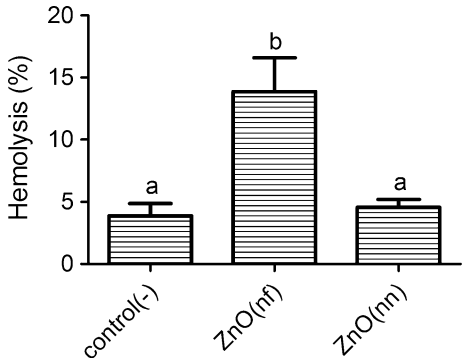

Fig. 7 Haemolysis of erythrocytes induced by ZnO nanoparticles. Erythrocyte suspensions (10 %, v/v) were incubated without (negative control) or with 0.1 mg/mL ZnO nanoflowers (nf) and nanoneedles (nn) in PBS at 37 °C for 24 h. The results are the mean and SEM of triplicate experiments. *Different letters* denote significant differences. One-way ANOVA and Tukey's multiple comparison test, $p < 0.05$

biological effects. For instance, there was higher bactericidal activity of platinum nanospheres compared to nanoflowers, which was explained by taking into account the higher accessibility of the nanospheres through the membrane pores (Gopal et al. 2013). In other research, no difference was observed between gold nanospheres and nanoflowers with respect to the reduction of de novo biosynthesis of RNA in nucleoli in breast cancer cells (Kodiha et al. 2014). In short, the higher cytotoxicity of ZnO nanoflowers compared to nanoneedles regarding the haemolytic effect is not similar to other model of cytotoxicity. Finally, we also take into account that the haemolytic effect could be still lower using whole blood, a model closer to the physiological condition, since the presence of human blood serum could deplete the ROS produced in the stimulatory process.

Studies on activation of neutrophils

Following our aims of studying the toxicity of ZnO nanoparticles in the blood components, the next target in this study was the neutrophil leukocytes. These cells are the predominant leukocytes in the blood and have the primary function of combating invading pathogens (Halliwell 2006). Neutrophils produce several reactive chemicals, such as superoxide radical anions, hydrogen peroxide and the potent microbicide, hypochlorous acid (Hampton et al. 1998). However, these oxidizing species are also involved in the host tissue damage, a process involved in the physiopathology of several inflammatory diseases (Mittal et al. 2014; Manda-Handzlik and Demkow 2015). For this reason, we evaluated the capacity of the nanoparticles to induce neutrophil activation.

First, we measured the capacity of the ZnO NPs to induce the release of superoxide radical anions by neutrophils. As a positive control, we used phorbol myristate acetate (PMA), which is a widely used soluble activator of neutrophil oxidative function via the protein kinase C (PKC) signalling pathway (Bertram and Ley 2011). The activation of neutrophil was evaluated by the light emission elicited by the reduction of lucigenin by superoxide radical anions, which is produced by the activation of the NADPH oxidase enzymatic complex in these cells (de Faria et al. 2012). Figure 8a shows the time-dependent light emission, highlighting the difference between the non-stimulated (negative control) and PMA-stimulated (positive control) neutrophils. The results also show that the nanoparticles were not able to increase the release of superoxide radical anions. In fact, a small decrease in the light emission in the presence of the nanoparticles is shown in Fig. 8a, but this was not statistically significant as shown in the replicates in Fig. 8b.

In the next assay with neutrophils, the production and release of H_2O_2 were evaluated. In this case, Amplex Red, a fluorescent probe specific for this reactive oxygen species (Zhou et al. 1997) was used to monitor the activation of the neutrophils. The results in Fig. 9 confirm the results as shown in Fig. 8, since the neutrophils were not activated by ZnO NPs.

Finally, we used the luminol-dependent chemiluminescence assay to monitor the activation of neutrophils by ZnO NPs. In contrast to the previous

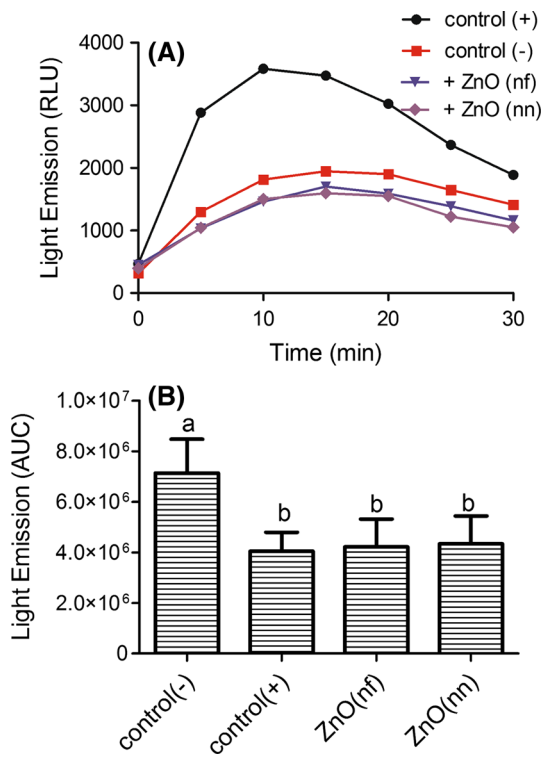

Fig. 8 Activation of neutrophils by ZnO nanoparticles (lucigenin assay). Neutrophils (1×10^6 cells/mL) were incubated without (negative control) or with 0.1 mg/mL ZnO nanoflowers (nf), nanoneedles (nn) and 10 μM lucigenin in PBS at 37 °C for 30 min. The positive control was obtained by adding 100 nM PMA. **a** Kinetic profile of light emission. **b** Total light emission. The results are the mean and SEM of triplicate experiments. *Different letters* denote significant differences. One-way ANOVA and Tukey's multiple comparison test, $p < 0.05$

assays, the luminol assay is non-specific for the reactive species as it is oxidized by several oxidizing agents, such as ozone, singlet oxygen and hydrogen peroxide in the presence of peroxidases (Khan et al. 2014). Moreover, and particularly important here, is the fact that hypochlorous acid produced by activated neutrophils is the main factor responsible for the luminol-dependent chemiluminescence in this cell-based assay (Aniansson et al. 1984). As hypochlorous acid is an important agent in tissue damage in chronic inflammatory diseases, this assay could reveal a potential deleterious effect of ZnO NPs. However, the activation of the neutrophils treated with ZnO NPs was not higher compared to the negative control cells. In fact, ZnO nanoflowers had some capacity to activate neutrophils, but statistically the activation was not different to the negative control and ZnO nanoneedles (Fig. 10).

There is some evidence of the direct effect of nanoparticles on neutrophils. Particularly relevant for our study was the demonstration that TiO_2, CeO_2 and ZnO NPs increased the expression of myeloperoxidase (Babin et al. 2013) and enhanced the phagocytosis capacity of neutrophils (Babin et al. 2015). Similarly, polyacrylic acid metal oxide nanoparticles (TiO_2, CeO_2, Fe_2O_3 and ZnO) increased the respiratory burst, i.e. the production of reactive oxygen species, by fish neutrophils (Ortega et al. 2015). However, although carboxy-functionalized ZnO NPs induced cell shape changes and activated phosphorylation, they did not induce the generation of reactive oxygen species in human neutrophils (Gonçalves and Girard 2014). These results are in agreement with our finding using nanoneedles and nanoflowers of ZnO.

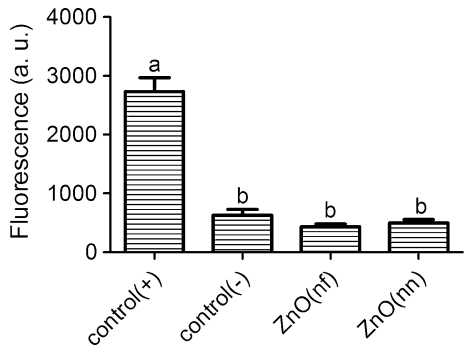

Fig. 9 Activation of neutrophils by ZnO nanoparticles (Amplex Red assay). Neutrophils (1×10^6 cells/mL) were incubated without (negative control) or with 0.1 mg/mL ZnO nanoflowers (nf), nanoneedles (nn) and 50 μM Amplex Red in PBS at 37 °C for 30 min. The positive control was obtained by adding 100 nM PMA. The results are the mean and SEM of triplicate experiments. *Different letters* denote significant differences. One-way ANOVA and Tukey's multiple comparison test, $p < 0.05$

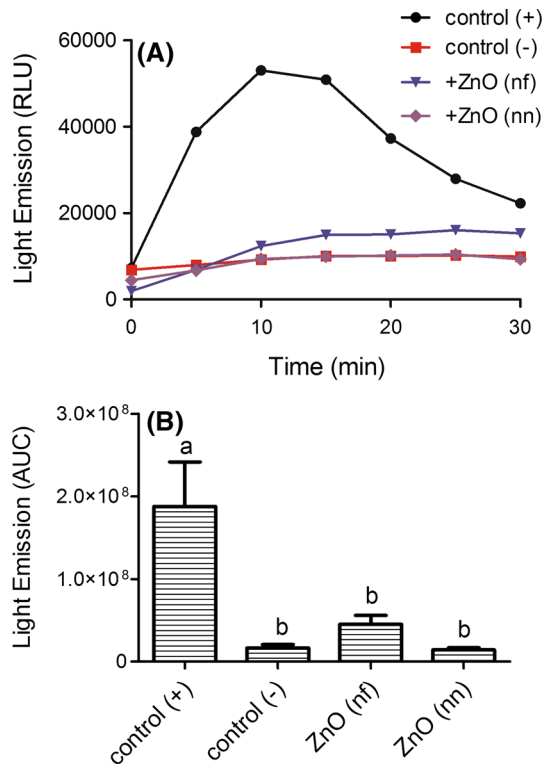

Fig. 10 Activation of neutrophils by ZnO nanoparticles (Luminol assay). Neutrophils (1×10^6 cells/mL) were incubated without (negative control) or with 0.1 mg/mL ZnO nanoflowers (nf), nanoneedles (nn) and 100 μM luminol in PBS at 37 °C for 30 min. The positive control was obtained by adding 100 nM PMA. **a** Kinetic profile of light emission. **b** Total light emission. The results are mean and SEM of triplicate experiments. *Different letters* denote significant differences. One-way ANOVA and Tukey's multiple comparison test, $p < 0.05$

Conclusions

Due to the wide biomedical applications of ZnO NPs, elucidation of their potential toxic properties is a hot topic. Here, we show the effect of ZnO NPs on blood components. Two different morphologies were synthesized and studied, namely, ZnO nanoneedles and ZnO nanoflowers. We found that neither type of NP induced structural alterations in HSA, including its capacity as a drug carrier. It is of note that although the

NPs were kept in contact with the protein for 24 h, there were no significant indications of denaturation. Similarly, the incubation of neutrophils with the NPs did not cause activation of these cells, as demonstrated by the absence of any significant release of reactive oxygen species. These findings suggest that these NPs are not able to trigger an inflammatory process. Finally, we tested whether NPs can induce haemolysis of erythrocytes. Unlike the previous assays, a small but statistically significant effect was observed for the nanoflower NPs, while nanoneedle NPs did not cause a haemolytic effect. However, we cannot discard that other factors like hydrodynamic size and charge density could also play a role in the induction of haemolysis. In conclusion, our results reinforce the concept that ZnO NPs are relatively safe for use in biomaterials. A potential exception is the capacity of nanoflower NPs to promote lysis of erythrocytes, a discovery that deserves further studies for clarification.

Acknowledgments This work was supported by Grants from the São Paulo Research Foundation (FAPESP, #2013/08784-0), National Council for Scientific and Technological Development (CNPq #440503/2014-0) and Coordination for the Improvement of Higher Education Personnel (CAPES).

Compliance with ethical standards

Conflict of interest The authors declare that they have no conflict of interest.

References

Aniansson H, Stendahl O, Dahlgren C (1984) Comparison between luminol- and lucigenin dependent chemiluminescence of polymorphonuclear leukocytes. Acta Pathol Microbiol Immunol Scand C 92:357–361

Babin K, Antoine F, Goncalves DM, Girard D (2013) TiO_2, CeO_2 and ZnO nanoparticles and modulation of the degranulation process in human neutrophils. Toxicol Lett 221:57–63

Babin K, Goncalves DM, Girard D (2015) Nanoparticles enhance the ability of human neutrophils to exert phagocytosis by a Syk-dependent mechanism. Biochim Biophys Acta 1850:2276–2282

Bertram A, Ley K (2011) Protein kinase C isoforms in neutrophil adhesion and activation. Arch Immunol Ther Exp (Warsz) 59:79–87

Bhogale A, Patel N, Sarpotdar P, Mariam J, Dongre PM, Miotello A, Kothari DC (2013) Systematic investigation on the interaction of bovine serum albumin with ZnO nanoparticles using fluorescence spectroscopy. Colloids Surf B Biointerfaces 102:257–264

Chia SL, Tay CY, Setyawati MI, Leong DT (2015) Biomimicry 3D gastrointestinal spheroid platform for the assessment of toxicity and inflammatory effects of zinc oxide nanoparticles. Small 11:702–712

Das D, Nath BC, Phukon P, Kalita A, Dolui SK (2013) Synthesis of ZnO nanoparticles and evaluation of antioxidant and cytotoxic activity. Colloids Surf B Biointerfaces 111:556–560

de Faria CM, Nazaré AC, Petrônio MS, Paracatu LC, Zeraik ML, Regasini LO et al (2012) Protocatechuic acid alkyl esters: hydrophobicity as a determinant factor for inhibition of NADPH oxidase. Curr Med Chem 19:4885–4893

Djurišić AB, Leung YH, Ng AM, Xu XY, Lee PK, Degger N, Wu RS (2015) Toxicity of metal oxide nanoparticles: mechanisms, characterization, and avoiding experimental artefacts. Small 11:26–44

Easo SL, Mohanan PV (2015) In vitro hematological and in vivo immunotoxicity assessment of dextran stabilized iron oxide nanoparticles. Colloids Surf B Biointerfaces 134:122–130

Fukui H, Iwahashi H, Endoh S, Nishio K, Yoshida Y, Hagihara Y, Horie M (2015) Ascorbic acid attenuates acute pulmonary oxidative stress and inflammation caused by zinc oxide nanoparticles. J Occup Health 57:118–125

Ghosh M, Chakraborty A, Mukherjee A (2013) Cytotoxic, genotoxic and the hemolytic effect of titanium dioxide (TiO_2) nanoparticles on human erythrocyte and lymphocyte cells in vitro. J Appl Toxicol 33:1097–1110

Giovanni M, Yue J, Zhang L, Xie J, Ong CN, Leong DT (2015) Pro-inflammatory responses of RAW264.7 macrophages when treated with ultralow concentrations of silver, titanium dioxide, and zinc oxide nanoparticles. J Hazard Mater 297:146–152

Gonçalves DM, Girard D (2014) Zinc oxide nanoparticles delay human neutrophil apoptosis by a de novo protein synthesis-dependent and reactive oxygen species-independent mechanism. Toxicol In Vitro 28:926–931

Gopal J, Hasan N, Manikandan M, Wu HF (2013) Bacterial toxicity/compatibility of platinum nanospheres, nanocuboids and nanoflowers. Sci Rep 3:1–8

Graciani FS, Ximenes VF (2013) Investigation of human albumin-induced circular dichroism in dansylglycine. PLoS One 8:e76849

Halliwell B (2006) Phagocyte-derived reactive species: salvation or suicide? Trends Biochem Sci 31:509–515

Hampton MB, Kettle AJ, Winterbourn CC (1998) Inside the neutrophil phagosome: oxidants, myeloperoxidase, and bacterial killing. Blood 92:3007–3017

Huang KL, Lee YH, Chen HI, Liao HS, Chiang BL, Cheng TJ (2015) Zinc oxide nanoparticles induce eosinophilic airway inflammation in mice. J Hazard Mater 297:304–312

Janotti A, Van de Walle CG (2009) Fundamentals of zinc oxide as a semiconductor. Rep Prog Phys 72:126501

Jeong SH, Kim HJ, Ryu HJ, Ryu WI, Park YH, Bae HC, Jang YS, Son SW (2013) ZnO nanoparticles induce TNF-α expression via ROS-ERK-Egr-1 pathway in human keratinocytes. J Dermatol Sci 72:263–273

Khan P, Idrees D, Moxley MA, Corbett JA, Ahmad F, von Figura G, Sly WS, Waheed A, Hassan MI (2014) Luminol-based chemiluminescent signals: clinical and non-clinical

application and future uses. Appl Biochem Biotechnol 173:333–355

Khorsand ZA, Majid WH, Wang HZ, Yousefi R, Moradi Golsheikh A, Ren ZF (2013) Sonochemical synthesis of hierarchical ZnO nanostructures. Ultrason Sonochem 20:395–400

Kitture R, Chordiya K, Gaware S, Ghosh S, More PA, Kulkarni P, Chopade BA, Kale SN (2015) ZnO nanoparticles-red sandalwood conjugate: a promising anti-diabetic agent. J Nanosci Nanotechnol 15:4046–4051

Kodiha M, Hutter E, Boridy S, Juhas M, Maysinger D, Stochaj U (2014) Gold nanoparticles induce nuclear damage in breast cancer cells, which is further amplified by hyperthermia. Cell Mol Life Sci 71:4259–4273

Lakowicz JR (2006) Principles of fluorescence spectroscopy, 3rd edn. Springer, Baltimore

Madhumitha G, Elango G, Roopan SM (2015) Biotechnological aspects of ZnO nanoparticles: overview on synthesis and its applications. Appl Microbiol Biotechnol 100:571–581

Manda-Handzlik A, Demkow U (2015) Neutrophils: the role of oxidative and nitrosative stress in health and disease. Adv Exp Med Biol 857:51–60

Miller JN (1979) Recent advances in molecular luminescence analysis. Proc Anal Div Chem Soc 16:203–208

Mittal M, Siddiqui MR, Tran K, Reddy SP, Malik AB (2014) Reactive oxygen species in inflammation and tissue injury. Antioxid Redox Signal 20:1126–1167

Ortega VA, Katzenback BA, Stafford JL, Belosevic M, Goss GG (2015) Effects of polymer-coated metal oxide nanoparticles on goldfish (*Carassius auratus* L.) neutrophil viability and function. Nanotoxicology 9:23–33

Paracatu LC, Faria CM, Quinello C, Rennó C, Palmeira P, Zeraik ML, da Fonseca LM, Ximenes VF (2014) Caffeic acid phenethyl ester: consequences of its hydrophobicity in the oxidative functions and cytokine release by leukocytes. Evid Based Complement Alternat Med 793629

Pillai GJ, Greeshma MM, Menon D (2015) Impact of poly(lactic-co-glycolic acid) nanoparticle surface charge on protein, cellular and haematological interactions. Colloids Surf B Biointerfaces 136:1058–1066

Quinlan GJ, Martin GS, Evans TW (2005) Albumin: biochemical properties and therapeutic potential. Hepatology 41:1211–1219

Roy R, Das M, Dwivedi PD (2015) Toxicological mode of action of ZnO nanoparticles: impact on immune cells. Mol Immunol 63:184–192

Sadjadpour S, Safarian S, Zargar SJ, Sheibani N (2015) Antiproliferative effects of ZnO, ZnO-MTCP and ZnO-CuMTCP nanoparticles with safe intensity UV and X-ray irradiation. Biotechnol Appl Biochem 63:113–124

Sahu D, Kannan GM, Vijayaraghavan R (2014) Size-dependent effect of zinc oxide on toxicity and inflammatory potential of human monocytes. J Toxicol Environ Health A 77:177–191

Santra MK, Banerjee A, Krishnakumar SS, Rahaman O, Panda D (2004) Multiple-probe analysis of folding and unfolding pathways of human serum albumin. Evidence for a framework mechanism of folding. Eur J Biochem 271:1789–1797

Saptarshi SR, Feltis BN, Wright PF, Lopata AL (2015) Investigating the immunomodulatory nature of zinc oxide nanoparticles at sub-cytotoxic levels in vitro and after intranasal instillation in vivo. J Nanobiotechnol 13:1–11

Sarkar A, Ghosh M, Sil PC (2014) Nanotoxicity: oxidative stress mediated toxicity of metal and metal oxide nanoparticles. J Nanosci Nanotechnol 14:730–743

Setyawati MI, Tay CY, Docter D, Stauber RH, Leong DT (2015a) Understanding and exploiting nanoparticles' intimacy with the blood vessel and blood. Chem Soc Rev 44:8174–8199

Setyawati MI, Tay CY, Leong DT (2015b) Mechanistic investigation of the biological effects of SiO_2, TiO_2, and ZnO nanoparticles on intestinal cells. Small 11:3458–3468

Sudlow G, Birkett DJ, Wade DN (1975) The characterization of two specific drug binding sites on human serum albumin. Mol Pharmacol 11:824–832

Sudlow G, Birkett DJ, Wade DN (1976) Further characterization of specific drug binding sites on human serum albumin. Mol Pharmacol 12:1052–1061

Tay CY, Setyawati MI, Xie J, Parak WJ, Leong DT (2014) Back to basics: exploiting the innate physico–chemical characteristics of nanomaterials for biomedical applications. Adv Funct Mater 24:5936–5955

Tripathy N, Ahmad R, Ko HA, Khang G, Hahn YB (2015) Enhanced anticancer potency using an acid-responsive ZnO-incorporated liposomal drug-delivery system. Nanoscale 7:4088–4096

Ximenes VF, Lopes MG, Petrônio MS, Regasini LO, Silva DH, da Fonseca LM (2010) Inhibitory effect of gallic acid and its esters on 2,2′-azobis(2-amidinopropane)hydrochloride (AAPH)-induced hemolysis and depletion of intracellular glutathione in erythrocytes. J Agric Food Chem 58:5355–5362

Yadollahi M, Gholamali I, Namazi H, Aghazadeh M (2015) Synthesis and characterization of antibacterial carboxymethyl cellulose/ZnO nanocomposite hydrogels. Int J Biol Macromol 74:136–141

Zhou M, Diwu Z, Panchuk-Voloshina N, Haugland RP (1997) A stable nonfluorescent derivative of resorufin for the fluorometric determination of trace hydrogen peroxide: applications in detecting the activity of phagocyte NADPH oxidase and other oxidases. Anal Biochem 253:162–168

Žūkienė R, Snitka V (2015) Zinc oxide nanoparticle and bovine serum albumin interaction and nanoparticles influence on cytotoxicity in vitro. Colloids Surf B Biointerfaces 135:316–323